Research article

THE DOMAIN STRUCTURE OF *Entamoeba* α-ACTININ2

BARBARA ADDARIO and LARS BACKMAN*
Department of Chemistry, Biochemistry, Umeå University, SE-901 87 Umeå,
Sweden

Abstract: *Entamoeba histolytica*, a major agent of human amoebiasis, expresses two distinct forms of α-actinin, a ubiquitous actin-binding protein that is present in most eukaryotic organisms. In contrast to all metazoan α-actinins, in both isoforms the intervening rod domain that connects the N-terminal actin-binding domain with the C-terminal EF-hands is much shorter. It is suggested that these α-actinins may be involved in amoeboid motility and phagocytosis, so we cloned and characterised each domain of one of these α-actinins to better understand their functional role. The results clearly showed that the domains have properties very similar to those of conventional α-actinins.

Key words: α-actinin, Spectrin repeat, Actin-binding protein

INTRODUCTION

The enteric protozoan parasite *Entamoeba histolytica* is the etiological agent of human amoebiasis. The parasite has a worldwide distribution, but it is most common in the tropical and subtropical areas of the world. It is estimated that *Entamoeba histolytica* infects 500 million humans annually, causes disease in 50 million and kills nearly 100,000 individuals every year [1-3]. Clinical manifestations vary from asymptomatic infection through diarrhoea, abdominal pain and dysentery to hepatitis, cysts, and amoebic liver, brain or lung abscesses [4-6]. The virulence of this pathogen is reflected in its ability to move, invade host tissues and phagocytose epithelial and red blood cells. Motility and phagocytosis are implicated in the virulence of the parasite, and are crucial for

* Author for correspondence. e-mail: lars.backman@chem.umu.se, tel.: (46) 90 786 5847, fax: (46) 90 786 7655

its pathogenesis [7, 8]. As both processes are driven by dynamic fluctuations of the cytoskeleton, much interest has been focused on the characterization of the *Entamoeba histolytica* actin-binding proteins [9-11] and the proteins involved in cytoskeletal reorganization [12-15].

The completion of the *E. histolytica* genome and its subsequent analysis have been crucial in revealing the key elements involved in the cytoskeleton dynamic and identifying the proteins involved in infection [16, 17]. Adhesion to the host cell requires a galactose/N-acetylgalactosamine inhibitable lectin (Gal/GalNAc lectin) [18] and cysteine proteases [19, 20] in addition to actin-binding proteins and a reorganization of the cytoskeleton [12, 21-23]. Analyses of potential interacting partners of the Gal/GalNAc lectin showed that two proteins rich in glutamic acid and lysine [24] and an α-actinin-like protein are attached to the lectin [9]. In many organisms, α-actinins are responsible for the attachment of the cytoskeleton to the plasma membrane through direct or indirect interactions with transmembrane proteins. Therefore, it is likely that either of the *Entamoeba* α-actinins (or both) has a similar function and is involved the infectious mechanism of the parasite.

α-actinins are ubiquitously actin-binding proteins, belonging to the spectrin superfamily. This group of proteins is characterized by the presence of a highly conserved N-terminal actin-binding domain, a central rod domain and a calcium-binding C-terminus [25-27]. Previously, we identified, cloned and characterized two *Entamoeba* α-actinins (63 kDa and 70 kDa) [28, 29]. These two isoforms display an unusual feature in their domain architecture: the rod domain is shorter and contains only one or two spectrin repeats, not four repeats as in all previous characterized α-actinins. Despite the shorter rod domain, both isoforms have conserved the ability to cross-link actin filaments in a calcium-sensitive manner.

Evolutionary studies of α-actinin have shown that the rod domain, important for homodimer formation, is less well conserved than the other domains. Not only does its amino acid composition vary between different α-actinin isoforms, but the number of spectrin repeats also differs in different species [30]. To better understand the role of the rod domain in actin bundling and cytoskeletal organization, we cloned and characterised the structural domains of *Entamoeba histolytica* α-actinin2.

MATERIALS AND METHODS

Cloning, expression and purification
The actin-binding domain (ABD; nucleotides 1-753, residues 1-251), the central rod region containing the spectrin-like repeats (ROD; nucleotides 754-1431, residues 252-477), and the ABD-ROD (nucleotides 1-1431, residues 1-477) and ROD-EF (nucleotides 754-1857, residues 252-619) were amplified by PCR using the full-length *E. histolytica* α-actinin2 (accession number: XM_648191) as the template (Fig. 1). The primers used for amplification contained BamHI

and XhoI restriction sites to allow directional ligation into the expression vector. A detailed list of the specific primers used for the amplification of the constructs is given in Tab. 1.
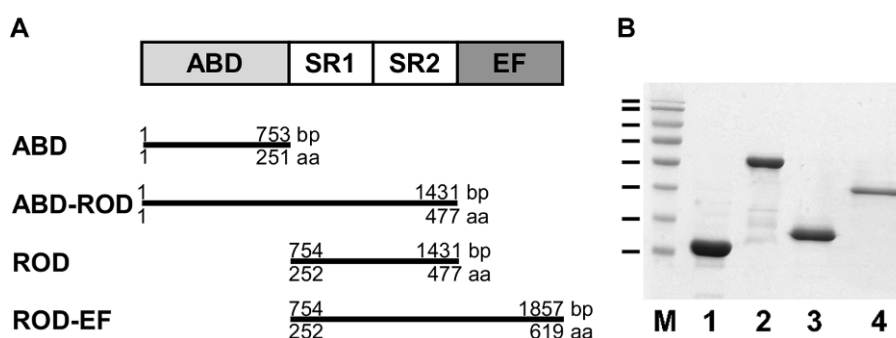

Fig. 1. The domain organization of *E. histolytica* α-actinin2 and its truncated mutants. A – The full-length protein contains an N-terminal actin-binding domain (ABD), a central rod (ROD) domain composed of two spectrin repeats (SR1 and SR2), and a C-terminal calcium-binding domain (EF). bp – base pair, aa – amino acid residues. B – SDS-PAGE analysis of recombinant peptides. Lane 1: ABD; lane 2: ABD-ROD; lane 3: ROD; lane 4: ROD-EF; lane M: molecular weight markers (from the top: 170, 130, 95, 72, 55, 43, 34 and 26 kDa).

Tab. 1. The primers used for the PCR amplification of the used constructs.

ABD	Forward	5'-TTTGGATCCATGGCTGATAGTGAGTTAGTTGCTC
	Reverse	5'-TTTCTCGAGCTATTATGTAGCTCTAAGGAAATCAAGG
ABD-ROD	Forward	5'-TTTGGATCCATGGCTGATAGTGAGTTAGTTGCT
	Reverse	5'-TTTCTCGAGCTATTATGCTTCATTAATTTGGG
ROD	Forward	5'-TTTGGATCCGAAGGTATGGTTCATGATTATG
	Reverse	5'-TTTCTCGAGCTATTATGCTTCATTAATTTGGG
ROD-EF	Forward	5'-TTTGGATCCGAAGGTATGGTTCATGATTATG
	Reverse	5'-TTTCTCGAGTTAATTAGTCTTAACCCAAGCAGC
NGFP-EH2	Forward	5'-AATAATCTCGAGCATGGCTGATAGTGAGTTA
	Reverse	5'-AATAATGGATCCTTAATTAGTCTTAACCCAAGC
EH2-CGFP	Forward	5'-AATAATCCATGGCTATGGCTGATAGTGAGTTA
	Reverse	5'-AATAAGACGTCCCATTAGTCTTAACCCAAGC
NGFP-lectin	Forward	5'-AATAATCTCGAGCAATAATGTTGGAGCTATT
	Reverse	5'-AATAATGGATCCTTATCCATTGAATGTTGCTGC
lectin-CGFP	Forward	5'-AATAATCCATGGCTAATAATGTTGGAGCTATT
	Reverse	5'-AATAAGACGTCCCTCCATTGAATGTTGCTGC

The restriction cleavage sites are underlined. All of the constructs of α-actinin2 were obtained by PCR using the full-length gene as the template.

The amplified fragments were digested and cloned into the BamHI and XhoI sites of a modified pET-19b vector containing a TEV-protease cleavage site and an N-terminal His10-tag. All of the nucleotide sequences were confirmed by sequence analysis at Eurofins MWG GmbH.

The purified plasmids were used to transform the *E. coli* BL21 (DE3) competent cells by heat shock. The transformed cells were grown in Luria-Bertani (LB) medium containing 100 μg/ml carbencillin at 37ºC until an optical density of 0.6-0.8 at 600 nm was obtained. The protein expression was induced by adding isopropyl thio-β-d-galactoside (IPTG) to a final concentration of 0.5 mM. After overnight expression (16 h) at 23ºC, the cells were harvested by centrifugation (29,000 x g for 15 min) and resuspended in NaPB (25 mM sodium phosphate buffer, pH 7.6, 150 mM NaCl) containing 1% Triton X-100.

For purification, the suspended cells were lysed by sonication. The cell debris was removed by centrifugation and the clear supernatant loaded onto a HisTrap™ Chelating HP column (GE Healthcare) charged with nickel. After eluting the unbound protein, the bound proteins were eluted with a gradient to 500 mM imidazole in NaPB. The imidazole eluate was dialyzed against 50 mM Tris-HCl, pH 7.6, and incubated at 4ºC for 16 h with Tobacco etch virus (TEV) protease (kindly provided by Dr David S. Waugh). The released His-tag and the His-tagged TEV protease was then removed by passing the dialysate through a second nickel-charged chelating column. When necessary, ion exchange chromatography on a HiTrap Q column (GE Healthcare) was performed to remove any remaining impurities. In this case, the target protein was eluted from the column using a salt gradient (1 M NaCl) in 50 mM Tris-HCl, pH 7.6.

The protein concentration was determined from the absorbance at 280 nm and using the molar absorptivity, calculated from the amino acid sequence [31]. The purity of the expressed peptides was routinely checked under denaturing conditions using SDS-polyacrylamide gel electrophoresis [32] (Fig. 1).

A Sephacryl S-400 HR column (0.66 x 37 cm, GE Healthcare) equilibrated with NaPB was used for gel filtration chromatography. Ferritin (440 kDa, 6.1 nm), lactate dehydrogenase (140 kDa, 4.2 nm), bovine serum albumin (67 kDa, 3.55 nm) and chymotrypsinogen (25 kDa, 2.09 nm) were used as protein molecular mass markers. Ferritin eluted very close to the void volume of this column.

Rabbit skeletal muscle actin was prepared from acetone powder as described by Spudich and Watt [33].

Actin co-sedimentation assay

Binding to actin was determined by a co-sedimentation assay using rabbit skeletal muscle actin in G-buffer (5 mM Tris-HCl, pH 8.0, 0.2 mM ATP, 0.5 mM β-mercaptoethanol). Actin polymerisation was initiated by adding KCl and $MgCl_2$ to respective final concentrations of 100 mM and 1 mM.

Monomeric actin and varying concentrations of ABD or ABD-ROD (with or without the His tag) were mixed in G-buffer, then KCl and $MgCl_2$ were added to a final volume of 150 μl to initiate polymerisation. After incubation for 1 h at

room temperature, the reaction mixture was either centrifuged at 13,000 rpm (16,000 x g) for 15 min (bundling assay) or at 90,000 rpm (350,000 x g) for 60 min (binding assay), and equal volumes of the supernatants and pellet were separated and analyzed by 12% SDS-PAGE. Coomassie-stained gels were scanned and quantified using TotalLab TL100 (Nonlinear Dynamics Ltd.).

Circular dichroism (CD) spectroscopy
The thermal stability was determined by CD spectroscopy. A Jasco J-810 spectrometer was used to collect spectra between 200 and 260 nm in NaPB using a 1-cm cuvette. The temperature was increased in steps of 2ºC, using a temperature gradient of 1ºC/min. The mean residue molar ellipticity ($[\Theta]_{MRW}$) at 222 nm was determined from three accumulated spectra and used for analysis. The transition temperature T_m was determined by fitting equation 1

$$\Theta = \frac{a_N + b_N \cdot T + \left(a_D + b_D \cdot T\right) 10^{m \cdot (T - T_m)}}{1 + 10^{m \cdot (T - T_m)}} \qquad (1)$$

where Θ is the observed ellipticity, $a_N + b_N \cdot T$ and $a_D + b_D \cdot T$ are the respective baselines for the folded and unfolded states, and m is the linear dependencies of the temperature [34].
The web service MLRC [35] at Pôle Bioinformatique Lyonnaise was used to predict the secondary structure. The α-helical content was also calculated using the relation $(-[\Theta_{222}] + 3000)/39000$ [36] as well as using the program CDNN [37].

Electron microscopy
Samples containing either 5 μM F-actin alone or mixed with different concentrations (2.5, 5 and 10 μM) of ABD or ABD-ROD were incubated for 1 h under the conditions described for the actin co-sedimentation experiment. The samples were added to formvar copper-coated grids, incubated for 3 to 5 min, negatively stained for 10 sec with 1% sodium silicotungstate (pH 7), dried, and imaged using a JEOL 1230 electron microscope.

GFP reassembly assay
The genes of the full-length *E. histolytica* α-actinin2 and the C-terminal part of the Gal/GalNAc lectin (provided by Dr. Nancy Guillén) were amplified by PCR using specific primers containing restriction sites for BamHI and XhoI, for insertion into the pET11a-link-NGFP vector, or for NcoI and AatII, for insertion into the pMRBAD-link-CGFP vector (see Tab. 1). The PCR products and vectors were digested and the ligated vectors were used to transform *E. coli* DH5α by electroporation. Colonies growing on LB medium containing either 100 μg/ml carbencillin (pET11a) or 35 μg/ml kanamycin (pMRBAD) were selected, cultured and used for plasmid preparation. Purified plasmids were sequenced to confirm that the inserts were correct and in the right reading frame.

E. coli BL21 (DE3) cells were co-transformed by electroporation and spread on LB agar plates, containing 100 μg/ml carbencillin and 35 μg/ml kanamycin. The plates were incubated at room temperature (20ºC) for 24 h. Single colonies were then picked and streaked on screening LB plates containing 100 μg/ml carbencillin, 35 μg/ml kanamycin and 10 μM IPTG and 0.2% (w/v) arabinose. The cells were grown at for 16 h at 30ºC followed by 1-3 days at 25ºC [38].

RESULTS AND DISCUSSION

Expression and purification

In order to characterize the different domains, primer pairs were designed to amplify the desired fragments of the *E. histolytica* α-actinin2 gene (Fig. 1). The amplified fragments were ligated into a modified pET vector with an N-terminal deca-histidine tag to facilitate purification. All of the constructs expressed high levels of stable and soluble recombinant peptides that could easily be purified by metal chelate chromatography, and when necessary, any remaining impurities were removed using ion exchange chromatography.

The molecular weights of the expressed peptides estimated from Coomassie stained gels (Fig. 1) were in good agreement with those calculated from the amino acid sequences (Tab. 2).

Tab. 2. Properties of the expressed peptides.

Domain	Size		$[\Theta_{222}]_{MRW}$ degrees cm^2 dmol^{-1} residue^{-1}	α-helix[b] %	α-helix[c] %	α-helix[d] %	Dimer formation
	Calculated kDa	SDS-PAGE[a] kDa					
ABD	28.4	28	15990	48.7	50.2	54.1	no
ROD	25.8	30	24888	71.5	77.1	75.9	yes
ABD-ROD	54.2	57	17470	52.5	55.9	63.9	yes
ROD-EF	41.6	44	21680	63.3	65.4	66.5	yes

[a]Molecular sizes were estimated from 12% SDS-PAGE. [b]The α-helical content determined as: $(-[\Theta_{222}]_{MRW} + 3000)/39000$ [36]. [c]The α-helical content was determined using the program CDNN [37]. [d]MLRC [35] at Pôle Bioinformatique Lyonnaise was used to predict the secondary structure.

Far-UV CD spectroscopy was used to analyze the secondary structure elements of the recombinant peptides. The results shown in Fig. 2 demonstrate that all of the peptides exhibited a spectrum with two negative peaks, at 208 and 222 nm, a typical characteristic of proteins rich in α-helical structures. This indicates that all of the peptides were properly folded. Furthermore, the determined α-helical content of each peptide corresponded very well with the values predicted by the secondary structure analysis (Tab. 2).
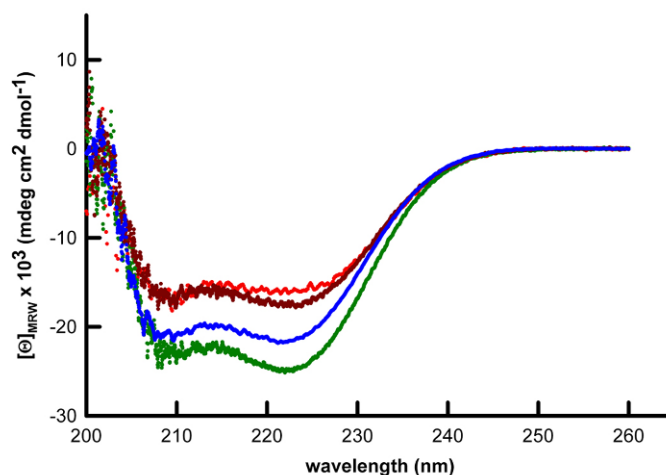
Fig. 2. Far-UV CD spectra. The far-UV CD spectra of 1.8 μM ABD (red), 1.2 μM ABD-ROD (dark red), 2.0 μM ROD (green) and 1.9 μM ROD-EF (blue) of *Entamoeba* α-actinin2 in 25 mM sodium phosphate, 150 mM NaCl, pH 7.6. The mean residue molar ellipticity was determined from 3 accumulated scans between 200 and 260 nm at 25ºC.

Dimer formation and thermal stability

It is well known that full-length α-actinin forms anti-parallel homodimers, with a globular ABD at each end of the dimer [25-27]. It is also known that due to the dimerisation and elongated shape, α-actinin behaves like a much larger molecule when analyzed by gel filtration. When passed through a Sephacryl S400 HR column, full-length *Entamoeba* α-actinin2 eluted very close to a globular reference protein of 440 kDa, with a Stokes radius of 6.1 nm. Considering the shorter rod domain [28], this value compares favourably with the previously determined radii of chicken skeletal muscle and sea urchin α-actinins (7.7 nm) [39] and that of Acanthamoeba (7.4 nm) [40], which all have a longer rod domain composed of four spectrin repeats.

The expressed peptides, with the exception of the ABD, eluted much earlier from the gel filtration column than expected for globular molecules of similar size (Fig. 3). Since the presence of the rod domain give the peptides an elongated shape, this was not surprising. However, when we compared the elution patterns with that for a spectrin peptide (composed of two spectrin repeats and an SH3 domain) of similar size (35.4 kDa) and shape, it was evident that the ABD-ROD, ROD and ROD-EF behaved as much larger molecules. The determined Stokes radii of these peptides (5.4, 5.2 and 5.7 nm, respectively) were much larger than that of the spectrin peptide (~4.3 nm), clearly indicating that ABD-ROD, ROD and ROD-EF formed homodimers (or even higher oligomers). Since the common denominator of the dimer-forming peptides is the presence of a rod domain, it seems reasonable to assume that the spectrin repeats present in the central rod domain are essential for the dimerisation of ABD-ROD, ROD and ROD-EF and that of full-length *Entamoeba* α-actinin2.
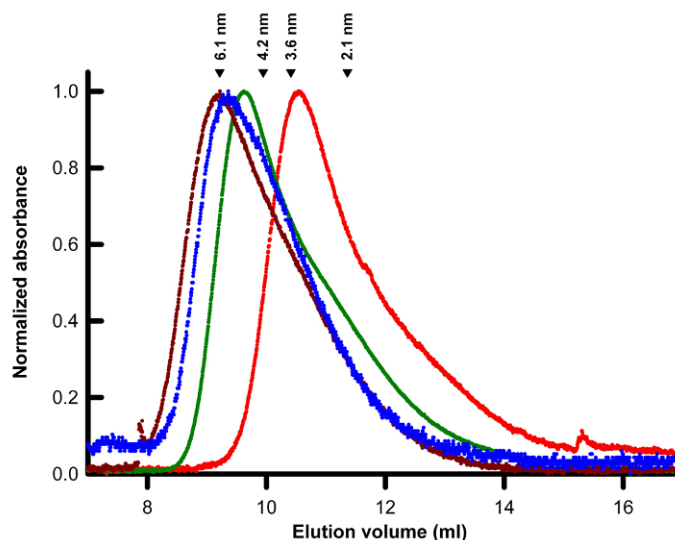
Fig. 3. Gel filtration. The apparent sizes of ABD (red), ABD-ROD (dark red), ROD (green) and ROD-EF (blue) were determined by gel filtration on a Sephacryl S400 HR column, equilibrated with 25 mM sodium phosphate buffer, pH 7.6, and 150 mM NaCl. Ferritin (440 kDa, 6.1 nm), lactate dehydrogenase (140 kDa, 4.2 nm), bovine serum albumin (67 kDa, 3.55 nm) and chymotrypsinogen (25 kDa, 2.09 nm) were used as reference proteins.
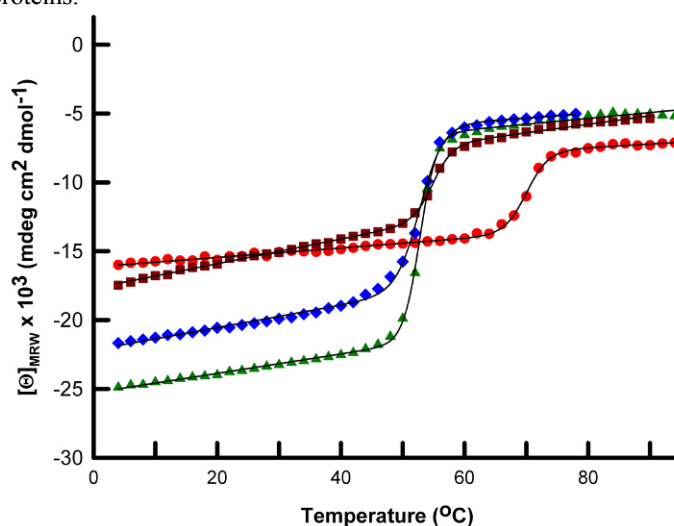

Fig. 4. Thermal stability. The thermal stabilities of ABD (red circles), ABD-ROD (dark red squares), ROD (green triangles) and ROD-EF (blue diamonds) were determined from the mean residue molar ellipticity at 222 nm.

The thermal stabilities of the peptides differed greatly. ABD was most stable with a transition temperature of 70ºC, whereas the other three peptides melted at much lower temperatures, as shown in Fig. 4. The transition temperature of the

ROD and ROD-EF peptides, with their two spectrin repeats, was close to 53ºC. By adding the actin-binding domain (ABD-ROD) the stability increased by 2ºC. Since these three peptides form dimers, it is possible that this increased the stability to some extent. Even though the peptides unfolded at different temperatures, they did so in a fairly narrow temperature range, indicating a very cooperative unfolding process of all four peptides, although the actin-binding domain-containing peptides displayed slightly less cooperativity than ROD and ROD-EF. All of the unfolding profiles displayed a single transition indicating that the folding process of each peptide follows a two-state behaviour.

It was previously shown that the stability of peptides containing two spectrin repeat units is very much dependent on the particular repeats. For instance, peptides comprising repeats 1 and 2 or 2 and 3 of human erythroid α-spectrin have transitions at 50 and 56ºC, respectively [41]. Similar tandem-repeats of repeats 3 and 4 and 7 and 8 of α-spectrin and of repeats 9 and 10 of β-spectrin all have transitions below 40ºC [42]. However, in contrast to our results, those authors observed two resolved phases in the unfolding process, indicating that the repeat units in these tandem-repeats were more or less independent of each other.

Actin binding

The actin-binding and actin-bundling properties of ABD and ABD-ROD were investigated using a co-sedimentation assay. The rationale of this assay is that a high-speed centrifugation will co-sediment actin filaments and any associated proteins (binding assay), whereas a low-speed centrifugation will only pellet cross-linked or bundled actin filaments (bundling assay).

As shown in Fig. 5, after a high-speed centrifugation ABD is present in the pelleted fraction, indicating that it has affinity for actin filaments. In the absence
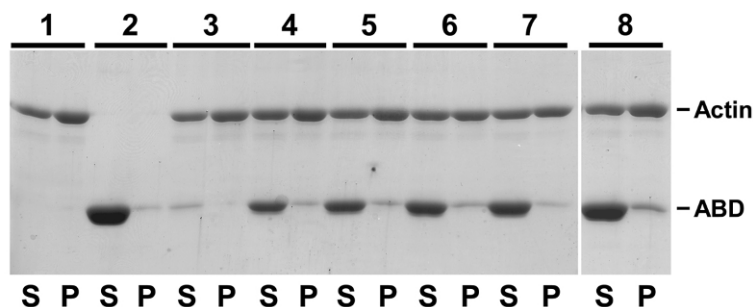

Fig. 5. High-speed co-sedimentation assay. Actin and *Entamoeba* ABD were centrifuged alone or together at different concentrations. After centrifugation (350,000 x g for 60 min), the supernatant (S) and the pellet (P) were separated on 12% SDS-PAGE. Lane 1: 5.0 μM actin; lane 2: 8.5 μM ABD; lane 3: 5.0 μM actin and 2 μM ABD; lane 4: 5.0 μM actin and 2.5 μM ABD; lane 5: 5.0 μM actin and 3 μM ABD; lane 6: 5.0 μM actin and 3.5 μM ABD; lane 7: 5.0 μM actin and 5 μM ABD-ROD; lane 8: 5.0 μM actin and 8.5 μM ABD.
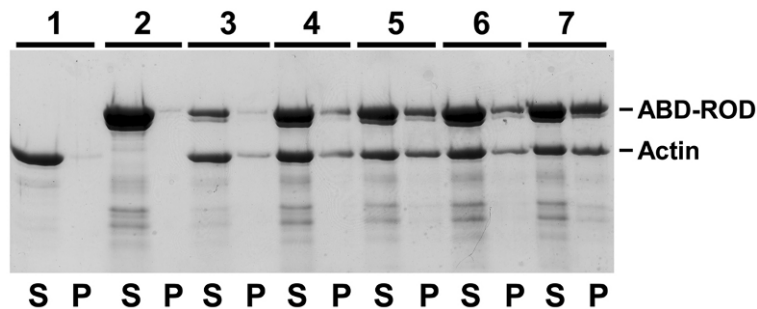
Fig. 6. Low-speed co-sedimentation assay. Actin and *Entamoeba* ABD-ROD were centrifuged alone or together at different concentrations. After centrifugation (16,000 x g for 15 min), the supernatant (S) and the pellet (P) were separated on 12% SDS-PAGE. Lane 1: 5.0 µM actin; lane 2: 8.5 µM ABD-ROD; lane 3: 5.0 µM actin and 2 µM ABD-ROD; lane 4: 5.0 µM actin and 5 µM ABD-ROD; lane 5: 5.0 µM actin and 6 µM ABD-ROD; lane 6: 5.0 µM actin and 7 µM ABD-ROD; lane 7: 5.0 µM actin and 8.5 µM ABD-ROD.
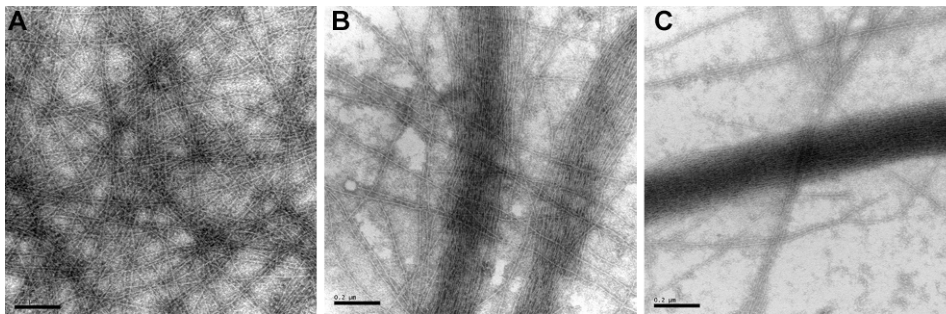

Fig. 7. Electron transmission microscopy. 4.5 µM actin was incubated with 10 µM *Entamoeba* ABD (A) or with 2.5 µM (B) or 5.0 µM (C) *Entamoeba* ABD-ROD before electron microscopy, as described in the Material and Methods section. Samples were added to the grids and negatively stained with sodium silicotungstate. A sepia tone was added to the micrographs to improve contrast. Bar: 200 nm.

of polymerised actin, no ABD was detected in the pelleted fraction, as expected. The low-speed assay showed that the actin-binding domain is not capable of cross-linking or bundling actin filaments.

Since ABD-ROD forms dimers, it was expected that it also should be able to cross-link or bundle actin filaments due to the presence of two actin-binding domains. This was tested using the bundling assay. In the presence of actin filaments both actin and the ABD-ROD peptide were recovered in the pellet after the low-speed centrifugation (Fig. 6). The amount of actin recovered in the pelleted fraction also increased with increasing concentrations of ABD-ROD.

The interaction between the ABD-ROD peptide and actin filaments was visualized by negative staining electron transmission microscopy (Fig. 7). At all

the tested ratios of ABD-ROD to actin, bundles were observed, but the higher the ratio, the denser the bundles. These very dense bundles appeared very similar to those observed with full length α-actinin2 [28]. When actin filaments were incubated with ABD, no bundles could be seen. At high concentrations of ABD (8.5 μM), we observed that a few (less than 5) filaments appeared to be organised in a parallel fashion.

Interaction with the Gal/GalNAc lectin
Previous studies have suggested that an α-actinin-like protein in *Entamoeba* binds directly to a lectin and that this interaction is required for adhesion [9]. To explore this interaction, we used a GFP fragment reassembly screen to detect the interaction between α-actinin2 and the lectin [38]. In this assay, the prey fused to one half of the GFP is co-expressed in *E. coli* with the bait fused to the other half of the GFP. If prey and bait interact, GFP reassembly is facilitated and should be possible to detect under UV light. Independent of how the two halves of GFP were combined with the cytoplasmic domain of the lectin and α-actinin2, we could not detect any fluorescent signal from the growing cells. We also utilized the His-tag present in the expressed N-terminal half of GFP to purify any reassembled GFP complex. Again, no GFP signal was observed. Therefore, our results do not support the suggestion of a direct interaction between the full-length α-actinin2 and the lectin. However, we cannot exclude the possibility that α-actinin2 associates indirectly with the lectin via another protein. Although less likely, it is also not possible to exclude the possibility that the GFP fragments were unable to reassemble or interfered with the bait-prey interaction.

In conclusion, we have shown that *Entamoeba* α-actinin2, similarly to all other studied α-actinins, forms stable dimers and is therefore able to cross-link and bundle actin filaments. In addition, our results have shown that the rod domain is required for dimer formation.

REFERENCES

1. Vanacova, S., Liston, D.R., Tachezy, J. and Johnson, P.J. Molecular biology of the amitochondriate parasites, Giardia intestinalis, Entamoeba histolytica and Trichomonas vaginalis. **Int. J. Parasitol.** <u>33</u> (2003) 235-255.
2. WHO/PAHO/UNESCO. WHO/PAHO/UNESCO report. A consultation with experts on amoebiasis. Mexico City, Mexico 28-29 January, 1997. **Epidemiol. Bull.** <u>18</u> (1997) 13-14.
3. Haque, R., Huston, C.D., Hughes, M., Houpt, E. and Petri, W.A., Jr. Amebiasis. **N. Engl. J. Med.** <u>348</u> (2003) 1565-1573.
4. Stanley, S.L., Jr. Amoebiasis. **Lancet** <u>361</u> (2003) 1025-1034.

5. Espinosa-Cantellano, M. and Martinez-Palomo, A. Pathogenesis of intestinal amebiasis: from molecules to disease. **Clin. Microbiol. Rev.** 13 (2000) 318-331.
6. Santi-Rocca, J., Rigothier, M.C. and Guillen, N. Host-microbe interactions and defense mechanisms in the development of amoebic liver abscesses. **Clin. Microbiol. Rev.** 22 (2009) 65-75.
7. Guillen, N. Role of signalling and cytoskeletal rearrangements in the pathogenesis of Entamoeba histolytica. **Trends Microbiol.** 4 (1996) 191-197.
8. Meza, I., Talamas-Rohana, P. and Vargas, M.A. The cytoskeleton of Entamoeba histolytica: structure, function, and regulation by signaling pathways. **Arch. Med. Res.** 37 (2006) 234-243.
9. Vargas, M., Sansonetti, P. and Guillen, N. Identification and cellular localization of the actin-binding protein ABP-120 from Entamoeba histolytica. **Mol. Microbiol.** 22 (1996) 849-857.
10. Ebert, F., Guillen, N., Leippe, M. and Tannich, E. Molecular cloning and cellular localization of an unusual bipartite Entamoeba histolytica polypeptide with similarity to actin binding proteins. **Mol. Biochem. Parasitol.** 111 (2000) 459-464.
11. Bailey, G.B., Shen, P.S., Beanan, M.J. and McCoomer, N.E. Actin associated proteins of Entamoeba histolytica. **Arch. Med. Res.** 23 (1992) 129-132.
12. Coudrier, E., Amblard, F., Zimmer, C., Roux, P., Olivo-Marin, J.C., Rigothier, M.C. and Guillen, N. Myosin II and the Gal-GalNAc lectin play a crucial role in tissue invasion by Entamoeba histolytica. **Cell. Microbiol.** 7 (2005) 19-27.
13. Sahoo, N., Labruyere, E., Bhattacharya, S., Sen, P., Guillen, N. and Bhattacharya, A. Calcium binding protein 1 of the protozoan parasite Entamoeba histolytica interacts with actin and is involved in cytoskeleton dynamics. **J. Cell Sci.** 117 (2004) 3625-3634.
14. Vargas, M., Voigt, H., Sansonetti, P. and Guillen, N. Molecular characterization of myosin IB from the lower eukaryote Entamoeba histolytica, a human parasite. **Mol. Biochem. Parasitol.** 86 (1997) 61-73.
15. Jain, R., Santi-Rocca, J., Padhan, N., Bhattacharya, S., Guillen, N. and Bhattacharya, A. Calcium-binding protein 1 of Entamoeba histolytica transiently associates with phagocytic cups in a calcium-independent manner. **Cell. Microbiol.** 10 (2008) 1373-89.
16. Loftus, B., Anderson, I., Davies, R., Alsmark, U.C., Samuelson, J., Amedeo, P., Roncaglia, P., Berriman, M., Hirt, R.P., Mann, B.J., Nozaki, T., Suh, B., Pop, M., Duchene, M., Ackers, J., Tannich, E., Leippe, M., Hofer, M., Bruchhaus, I., Willhoeft, U., Bhattacharya, A., Chillingworth, T., Churcher, C., Hance, Z., Harris, B., Harris, D., Jagels, K., Moule, S., Mungall, K., Ormond, D., Squares, R., Whitehead, S., Quail, M.A., Rabbinowitsch, E., Norbertczak, H., Price, C., Wang, Z., Guillen, N., Gilchrist, C., Stroup, S.E., Bhattacharya, S., Lohia, A., Foster, P.G., Sicheritz-Ponten, T., Weber, C., Singh, U., Mukherjee, C., El-Sayed, N.M., Petri, W.A., Jr., Clark, C.G.,

Embley, T.M., Barrell, B., Fraser, C.M. and Hall, N. The genome of the protist parasite Entamoeba histolytica. **Nature** <u>433</u> (2005) 865-868.

17. Clark, C.G., Alsmark, U.C., Tazreiter, M., Saito-Nakano, Y., Ali, V., Marion, S., Weber, C., Mukherjee, C., Bruchhaus, I., Tannich, E., Leippe, M., Sicheritz-Ponten, T., Foster, P.G., Samuelson, J., Noel, C.J., Hirt, R.P., Embley, T.M., Gilchrist, C.A., Mann, B.J., Singh, U., Ackers, J.P., Bhattacharya, S., Bhattacharya, A., Lohia, A., Guillen, N., Duchene, M., Nozaki, T. and Hall, N. Structure and content of the Entamoeba histolytica genome. **Adv. Parasitol.** <u>65</u> (2007) 51-190.

18. Blazquez, S., Rigothier, M.C., Huerre, M. and Guillen, N. Initiation of inflammation and cell death during liver abscess formation by Entamoeba histolytica depends on activity of the galactose/N-acetyl-D-galactosamine lectin. **Int. J. Parasitol.** <u>37</u> (2007) 425-433.

19. Que, X. and Reed, S.L. Cysteine proteinases and the pathogenesis of amebiasis. **Clin. Microbiol. Rev.** <u>13</u> (2000) 196-206.

20. Moncada, D., Keller, K., Ankri, S., Mirelman, D. and Chadee, K. Antisense inhibition of Entamoeba histolytica cysteine proteases inhibits colonic mucus degradation. **Gastroenterology** <u>130</u> (2006) 721-730.

21. Tavares, P., Rigothier, M.C., Khun, H., Roux, P., Huerre, M. and Guillen, N. Roles of cell adhesion and cytoskeleton activity in Entamoeba histolytica pathogenesis: a delicate balance. **Infect. Immun.** <u>73</u> (2005) 1771-1778.

22. Marion, S., Laurent, C. and Guillen, N. Signalization and cytoskeleton activity through myosin IB during the early steps of phagocytosis in Entamoeba histolytica: a proteomic approach. **Cell. Microbiol.** <u>7</u> (2005) 1504-1518.

23. Santi-Rocca, J., Weber, C., Guigon, G., Sismeiro, O., Coppee, J.Y. and Guillen, N. The lysine- and glutamic acid-rich protein KERP1 plays a role in Entamoeba histolytica liver abscess pathogenesis. **Cell. Microbiol.** <u>10</u> (2008) 202-217.

24. Seigneur, M., Mounier, J., Prevost, M.C. and Guillen, N. A lysine- and glutamic acid-rich protein, KERP1, from *Entamoeba histolytica* binds to human enterocytes. **Cell. Microbiol.** <u>7</u> (2005) 569-579.

25. Sjöblom, B., Salmazo, A. and Djinovic-Carugo, K. Alpha-actinin structure and regulation. **Cell Mol Life Sci** <u>65</u> (2008) 2688-2701.

26. Blanchard, A., Ohanian, V. and Critchley, D. The structure and function of α-actinin. **J. Muscle Res. Cell Motil.** <u>10</u> (1989) 280-289.

27. Otey, C.A. and Carpen, O. α-actinin revisited: a fresh look at an old player. **Cell Motil. Cytoskeleton** <u>58</u> (2004) 104-111.

28. Virel, A., Addario, B. and Backman, L. Characterization of Entamoeba histolytica α-actinin2. **Mol. Biochem. Parasitol.** <u>154</u> (2007) 82-89.

29. Virel, A. and Backman, L. Characterization of Entamoeba histolytica α-actinin. **Mol. Biochem. Parasitol.** <u>145</u> (2006) 11-17.

30. Virel, A. and Backman, L. A comparative and phylogenetic analysis of the α-actinin rod domain. **Mol. Biol. Evol.** <u>24</u> (2007) 2254-2265.

31. Gill, S.C. and von Hippel, P.H. Calculation of protein extinction coefficients from amino acid sequence data. **Anal. Biochem.** <u>182</u> (1989) 319-326.
32. Laemmli, U.K. Cleavage of structural proteins during the assembly of the head of bacteriophage T4. **Nature** <u>227</u> (1970) 680-685.
33. Spudich, J.A. and Watt, S. The regulation of rabbit skeletal muscle contraction. Biochemical studies of the interaction of the tropomyosin-troponin complex with actin and the proteolytic fragments of myosin. **J. Biol. Chem.** <u>246</u> (1971) 4866-4871.
34. Petzold, K., Ohman, A. and Backman, L. Folding of the αII-spectrin SH3 domain under physiological salt conditions. **Arch. Biochem. Biophys.** <u>474</u> (2008) 39-47.
35. Guermeur, Y., Geourjon, C., Gallinari, P. and Deleage, G. Improved performance in protein secondary structure prediction by inhomogeneous score combination. **Bioinformatics** <u>15</u> (1999) 413-421.
36. Morrow, J.A., Segall, M.L., Lund-Katz, S., Phillips, M.C., Knapp, M., Rupp, B. and Weisgraber, K.H. Differences in stability among the human apolipoprotein E isoforms determined by the amino-terminal domain. **Biochemistry** <u>39</u> (2000) 11657-11666.
37. Böhm, G., Muhr, R. and Jaenicke, R. Quantitative analysis of protein far UV circular dichroism spectra by neural networks. **Protein Eng.** <u>5</u> (1992) 191-195.
38. Wilson, C.G., Magliery, T.J. and Regan, L. Detecting protein-protein interactions with GFP-fragment reassembly. **Nat. Methods** <u>1</u> (2004) 255-262.
39. Mabuchi, I., Hamaguchi, Y., Kobayashi, T., Hosoya, H. and Tsukita, S. Alpha-actinin from sea urchin eggs: biochemical properties, interaction with actin, and distribution in the cell during fertilization and cleavage. **J. Cell Biol.** <u>100</u> (1985) 375-383.
40. Wachsstock, D.H., Schwarz, W.H. and Pollard, T.D. Cross-linker dynamics determine the mechanical properties of actin gels. **Biophys. J.** <u>66</u> (1994) 801-809.
41. Menhart, N., Mitchell, T., Lusitani, D., Topouzian, N. and Fung, L.W.M. Peptides with more than one 106-amino acid sequence motif are needed to mimic the structural stability of spectrin. **J. Biol. Chem.** <u>271</u> (1996) 30410-30416.
42. An, X., Guo, X., Zhang, X., Baines, A.J., Debnath, G., Moyo, M., Salomao, M., Bhasin, N., Johnson, C., Discher, D., Gratzer, W.B. and Mohandas, N. Conformational stabilities of the structural repeats of erythroid spectrin and their functional implications. **J. Biol. Chem.** <u>281</u> (2006) 10527-10532.